arXiv:hep-ph/0211253v1 15 Nov 2002

What are we learning from RHIC?*

D. Kharzeev[a†]

[a]Nuclear Theory Group,
Physics Department,
Brookhaven National Laboratory,
Upton, New York 11973-5000, USA

This talk is an attempt to summarize some of the first results obtained at RHIC. I discuss the significance of these measurements for establishing the properties of hot and dense QCD matter and for understanding the dynamics of the theory at the high parton density, strong color field frontier.

1. Introduction

1.1. What is RHIC?

Relativistic Heavy Ion Collider (RHIC) at Brookhaven National Laboratory on Long Island, New York, began operation in 2000 culminating over ten years of development and construction, and a much longer period of theoretical speculations about the properties of hot QCD matter produced in nuclear collisions in the collider regime.

RHIC's 2.4-mile rings contain superconducting magnets, which operate at minus 451.6 degrees Fahrenheit, 4.5 degrees above the absolute zero. RHIC collides two intersecting heavy ion beams at center-of-mass energy of up to 200 GeV/A (at luminosity of up to $10^{26} sec^{-1} cm^2$, which can be further increased in the future), and polarized proton beams at c.m.s. energy of up to 500 GeV. The total energy in the gold–gold collision thus reaches 40 TeV, which is at present the World's record collision energy. In the *pp* mode, the unique possibility offered by RHIC for the first time is the study of double spin asymmetries and other spin observables.

1.2. RHIC experiments

There are currently five experiments at RHIC: BRAHMS, PHENIX, PHOBOS, STAR, which can operate in both heavy ion and *pp* mode, and PP2PP, which aims exclusively at the study of elastic and diffractive *pp* interactions. These experiments are different in their focus; however all of them also provide the information about the basic properties of the collisions. The data from different collaborations can thus be cross–correlated and independently verified.

*Invited talk given at the XX International Symposium on Lattice Field Theory "Lattice 2002", Cambridge, MA, June 24 - 29, 2002.
†Work supported by the U.S. Department of Energy under Contract No. DE-AC02-98CH10886.

The BRAHMS experiment is designed to measure charged hadrons over a wide range of rapidity and transverse momentum. PHENIX is a large versatile experiment designed to study the production of charged and neutral hadrons, leptons, and photons. The PHOBOS experiment is aimed at measuring the global properties of nuclear collisions, and at the study of fluctuations and correlations in the production of hadrons. STAR, one of the two large–scale RHIC experiments, focuses on measurements of the production of various hadron species over a large solid angle and is well suited, in particular, for the study of multi–particle correlations and fluctuations on the event–by–event basis.

1.3. RHIC physics: QCD

RHIC is a machine entirely dedicated to the study of Quantum Chromo–Dynamics – the theory of strong interactions. This includes the study of matter at unprecedented energy densities and understanding the structure of the proton, in particular, its spin composition. Since the spin program at RHIC at the time of this talk is at the very beginning, I will concentrate in this talk entirely on the heavy ion program.

Asymptotic freedom of QCD [1], [2] ensures that the dynamics of quarks and gluons at sufficiently high density can be addressed by weak coupling methods. This includes both the thermalized quark–gluon plasma at high temperature and the wave functions of the colliding nuclei described, at small Bjorken x, by parton saturation and the Color Glass Condensate [3, 4, 5, 6].

2. Looking at the first RHIC data

2.1. Global observables

Global observables are the most general characteristics of the collision, including particle multiplicity, its dependence on the centrality of the collision and on rapidity, and azimuthal distribution of the produced particles. The centrality is determined by the impact parameter in the collision; since this is not a quantity which can be measured directly, centrality is usually determined in terms of a certain cut in the multiplicity distribution; e.g., a $0-10\%$ centrality cut means that out of a given sample, 10% of the events which have the highest multiplicity have been selected. It is convenient to characterize centrality in terms of the number of "participants" – the nucleons which underwent an inelastic interaction in a given collision. Glauber theory [7] can be used to correlate a certain centrality cut with an average number of participants (for an explicit set of formulae for nuclear collisions, see e.g. [8], [9]). This procedure can be independently verified by measuring the energy carried forward by spectator neutrons; for that purpose all RHIC experiments are equipped by Zero Degree Calorimeters.

2.1.1. Multiplicity

Multiplicity in heavy ion collision tells us which fraction of the collision energy is inelastically transferred to secondary particles. Theoretical expectations for hadron multiplicities at RHIC varied by factor of five, and the experimental verdict was thus eagerly awaited. After the commissioning of the machine, the first multiplicity results did not take long to come; they are shown on Fig. 1 in comparison to the multiplicity previously measured in pp and $\bar{p}p$ collisions. The measured multiplicity appeared much smaller than most theoretical predictions. Is this disappointing? To answer this question, let us recall

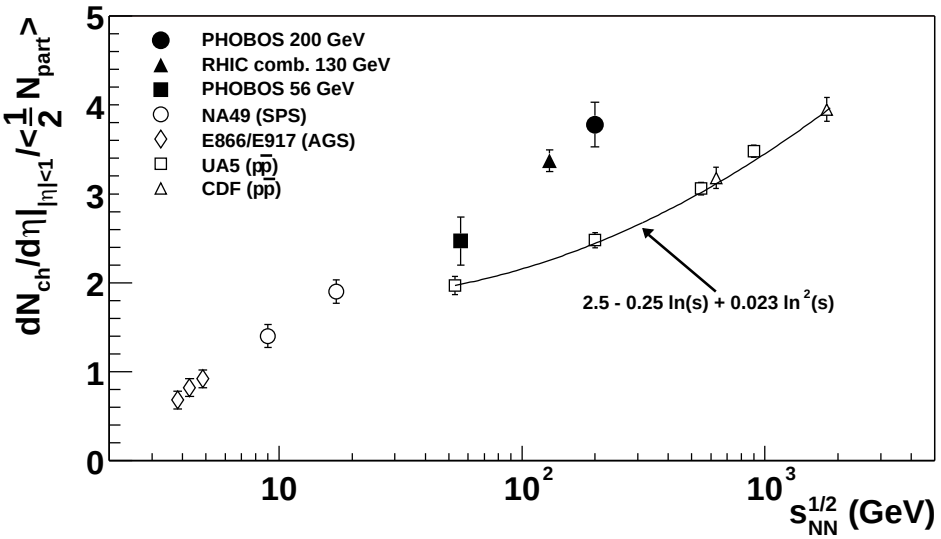

Figure 1. Charged multiplicity per participant pair in central Au Au collisions as measured at RHIC is compared to the multiplicity in pp and $\bar{p}p$ collisions; from [12].

that, by the very definition, an incoherent superposition of *independent* nucleon–nucleon collisions yields multiplicity equal to the number of collisions times the multiplicity in NN collision. This trivial statement holds also in the presence of elastic rescatterings. Indeed, according to so-called AGK cutting rules [10] of multiple scattering theory, the nuclear cross section is given by

$$E\frac{d^3\sigma^a_{AB}}{d^3p} = T_{AB}(\vec{b})E\frac{d^3\sigma^a_{NN}}{d^3p}, \tag{1}$$

where the nuclear overlap function is

$$T_{AB}(\vec{b}) = \int d^2s T_A(\vec{s})T_B(\vec{b}-\vec{s}), \tag{2}$$

and the nuclear thickness function $T_A(\vec{b}) = \int_{-\infty}^{\infty} dz \rho_A(\vec{b},z)$ is the integral over the nuclear density. Integration over impact parameter b yields

$$E\frac{d^3\sigma^a_{AB}}{d^3p} = AB\ E\frac{d^3\sigma^a_{NN}}{d^3p}, \tag{3}$$

and correspondingly the particle multiplicity would scale as

$$\frac{dn}{d\eta} = AB\ \frac{1}{\sigma^{in}_{AB}}\frac{d\sigma_{NN}}{d\eta}\ \sim A^{4/3}B^{4/3}\ \frac{dn_{NN}}{d\eta}. \tag{4}$$

Using the numbers of collisions ($\simeq 1050$) and participants ($\simeq 340$) in central ($0-6\%$ centrality cut) Au Au collisions from Glauber model calculations [9], we would thus conclude that $AuAu$ multiplicity per participant pair should exceed NN multiplicity by

factor of 3. Instead, the data at the highest RHIC energy of $\sqrt{s} = 200$ GeV show the difference of only about 50%. Given that any inelastic rescatterings in the final state can only increase the multiplicity, we therefore have an experimental *proof* of a high degree of coherence in multi-particle production in nuclear collisions at RHIC energies. The diagrams which allow to evade the AGK theorem are Gribov's "inelastic shadowing" corrections [11] which correspond to the excitation of high–mass intermediate states in multiple scattering; the process thus no longer can be decomposed in terms of elementary NN interactions. In parton language, these contributions correspond to multi–parton coherent interactions.

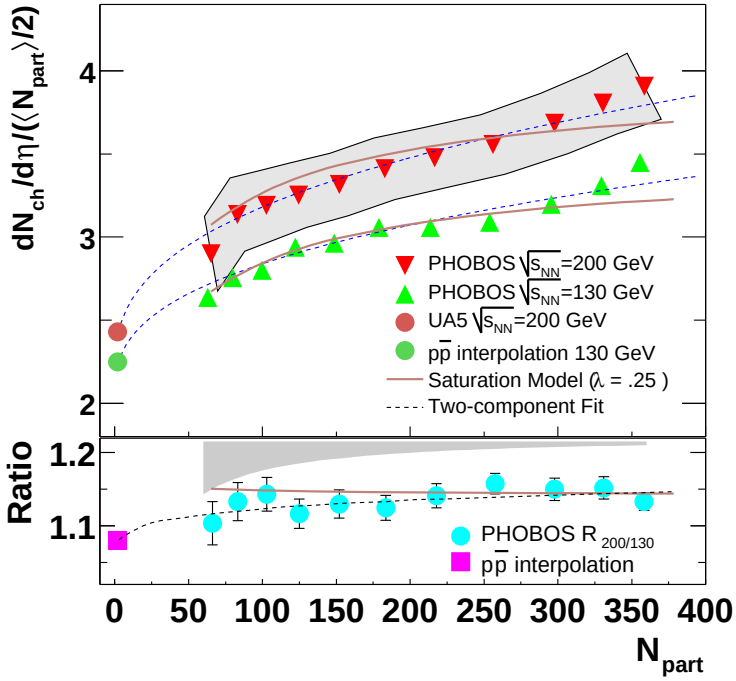

Figure 2. Centrality dependence of the charged particle multiplicity near mid-rapidity in Au + Au collisions at $\sqrt{s} = 130$ GeV and 200 GeV, from [13].

2.1.2. Centrality dependence

The dependence of multiplicity upon the number of participants discussed above can be established by selecting different centrality cuts. The result is shown in Fig.2; one can see that the multiplicity per participant pair increases with centrality, but not quite as fast as it would if the NN collisions were independent.

If we decompose the multiplicity measured in NN collisions at some energy $\sqrt{s}$ into a fraction $X(s)$ coming from "hard" processes, and the remaining fraction $1 - X(s)$ coming from "soft" processes, and assume that in nuclear collisions "hard" processes are incoherent and thus scale with the number of collisions, whereas "soft" processes scale

with the number of participants [14], we arrive at the following simple parameterization [9]

$$\frac{dn_{AA}}{d\eta} = [(1 - X(s))\ \langle N_{part}\rangle + X(s)\,\langle N_{coll}\rangle]\ \frac{dn_{NN}}{d\eta}, \tag{5}$$

which describes the data quite well. In the framework of perturbative QCD approach, one has to assume that the coefficient $X(s)$ is proportional to the mini–jet production cross section, and thus grows with energy reflecting the growth of the parton distributions at small Bjorken x, $X(s) \sim [xG(x)]^2$, with $x \sim 1/\sqrt{s}$. Therefore one expects [15] that the centrality dependence should become increasingly steep as the $\sqrt{s}$ increases (for the latest development, see however [16]). This increase is not seen in Fig.2, which in the lower panel shows that the ratio of the distributions at $\sqrt{s} = 200$ GeV and $\sqrt{s} = 130$ GeV is constant within error bars. The almost constant ratio appears consistent with the prediction [17],[9] based on the ideas of parton saturation, where the increase of multiplicity stems from the running of the QCD coupling constant determining the occupation number $\sim 1/\alpha_s$ of gluons in the classical field. The forthcoming results at $\sqrt{s} = 20$ GeV will further constrain the production dynamics.

2.1.3. Rapidity distributions

Distributions of the produced particles in the emission angle θ (with respect to the collision axis), or pseudo-rapidity $\eta = -\ln[\tan(\theta/2)]$ provide another important characteristic of the collision process. Two features of RHIC results (see Fig. 3) are especially noteworthy: i) the distributions do not exhibit scaling in η; ii) the deviation from NN results is maximal in the central rapidity region whereas the shapes of the AA and NN distributions are similar in the fragmentation region. Moreover, when corrected for the different beam rapidity $\eta \to \eta - y_{beam}$, distributions at different energies exhibit approximate scaling in the fragmentation region ("limiting fragmentation").

2.1.4. Azimuthal distributions

Of great interest and importance are the distributions of the produced hadrons in the azimuthal angle. Indeed, if all of the NN collisions were independent, there would be no reason to expect asymmetry in the distribution of the produced hadrons in the azimuthal angle (measured with respect to the reaction plane). This is why the azimuthal asymmetry represents a sensitive test of the collective effects in nuclear collisions. The azimuthal angle distributions of the produced hadrons are usually expanded in harmonics in the following way[3]:

$$\frac{dN}{d\varphi} = 1 + 2v_1 \cos\varphi + 2v_2 \cos 2\varphi + ... \tag{6}$$

Fig. 4 shows the extracted from RHIC data coefficient v_2 ($v_2 \neq 0$ in the language of the field corresponds to "elliptic flow"). One can see that the asymmetry of the azimuthal distribution is quite sizable, and for peripheral collisions (small multiplicity n_{ch}/n_{max}) reaches about 35%.

[3]The absence of the terms proportional to $\sin n\varphi$ is the consequence of parity conservation; it would be interesting to search for their presence in the data in view of the speculative scenarios allowing for P and CP violation in hot QCD [20].

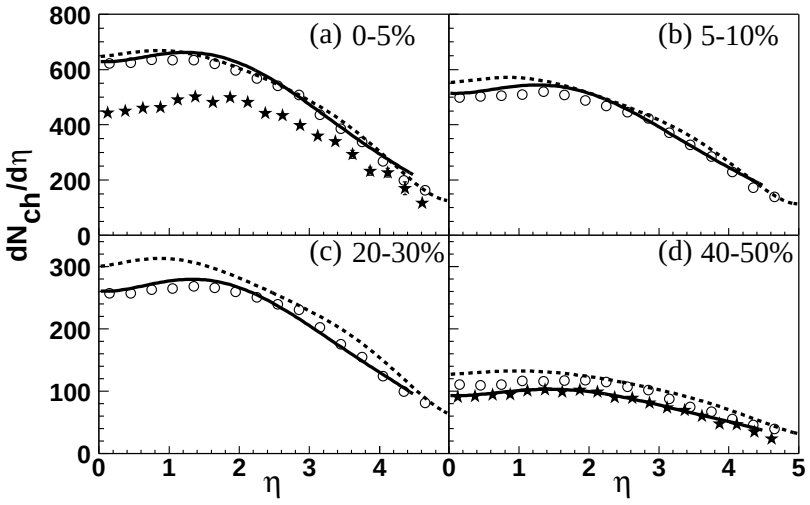

Figure 3. Pseudo-rapidity distributions of charged particles from Au + Au collisions at $\sqrt{s} = 200$ GeV (open circles), from [18]. Solid line is the prediction based on parton saturation [17], and dashed line is the multi-phase transport model calculation [19]. The $\bar{p}p$ distribution rescaled by $\langle N_{part}/2 \rangle$ is shown by stars.

This effect certainly indicates the presence of collectivity in nuclear collisions, and comes out quite naturally in hydrodynamical calculations which assume complete thermalization in the final state [22], [23]. However, final state effects are not the only possible origin of the azimuthal asymmetry; indeed, as we have discussed above, the high degree of coherence in the *initial* state signaled by the multiplicity measurements, in the parton saturation scenario, introduces strong correlation between the transverse momentum of the parton and its transverse coordinate in the wave functions of the nuclei. When the nuclei collide, this effect mimics at least a part of the asymmetry usually ascribed exclusively to final–state interactions [24], [25]. The magnitude of the elliptic flow which can originate from the coherence in the initial state is still a subject of ongoing research and debates.

The dependence of the elliptic flow on the transverse momentum of the hadrons presents a puzzle [21]; the value of v_2 is seen to first increase with p_t, and then saturate. This contradicts to hydrodynamics, predicting a monotonic increase of v_2 with p_t; of course hydrodynamics cannot be trusted at high p_t anyway because the density of hard particles is too small to allow for a meaningful statistical description. Energy loss of the produced jets can contribute to the azimuthal asymmetry at high p_t (see, e.g., [26]), even though it is not yet clear if the magnitude of the effect can be reproduced under realistic assumptions about the density of the medium and the jet interaction cross section [27].

2.1.5. Hadron abundances

The measurements of yields of different hadrons at RHIC hold many surprises. Of particular interest is the fact that even at RHIC energies the asymmetry between baryons

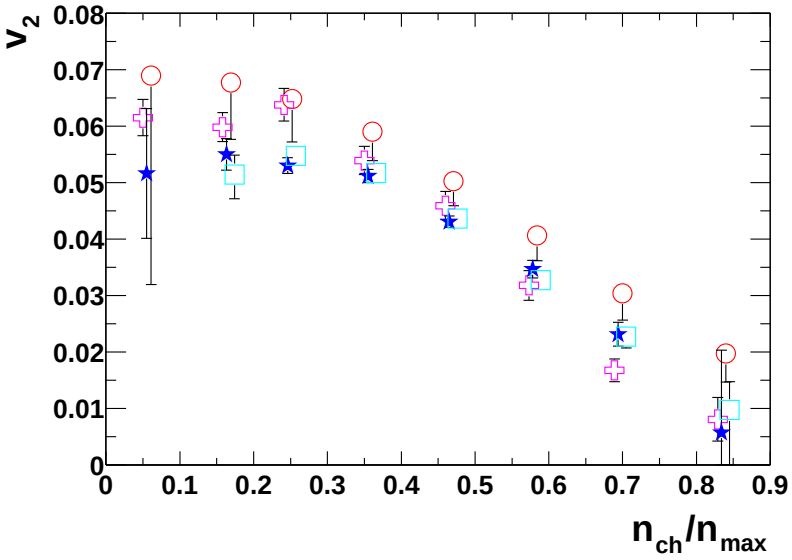

Figure 4. Azimuthal anisotropy of hadron production in Au + Au collisions at at $\sqrt{s} = 130$ GeV; v_2 is the weight of the second harmonic, $\cos 2\varphi$, in the particle distribution in the azimuthal angle φ; from [21].

and antibaryons is still sizable, with $\bar{p}/p$ ratio about 0.65 [28]. This signals the diffusion of baryon number to quite small values of Bjorken $x \sim 10^{-2}$.

2.2. Hard processes

2.2.1. Suppression of high p_t particles

Jet energy loss was among the first signatures suggested for the diagnostics of the hot quark–gluon matter [29, 30, 31]. This is why the measurements of the high p_t hadron production excited a lot of interest. Indeed, the experimental results are striking – as can be seen in Fig.5, the yield of high p_t hadrons is drastically reduced with respect to what is expected for incoherent production in NN collisions. This behavior is very different from what was previously observed in $Pb - Pb$ collisions at CERN SPS and in $\alpha - \alpha$ collisions at CERN ISR (see Fig.5). Does this important discovery signal jet energy loss in the quark–gluon plasma? The answer to this question can be given after we know the results of the forthcoming measurements in $p(d)A$ collisions, which would allow to separate clearly the effects coming from the initial state.

2.2.2. B/π puzzle

Another striking puzzle at RHIC is a rapid increase of the baryon–to–pion ratio in central $Au - Au$ collisions at high p_t [33]. The growth of this ratio is expected in the hydrodynamical scenario, in which equal velocity of the expanding parton "fluid" implies higher transverse momentum for more massive particles. However, the validity of hydrodynamical description is dubious at high p_t where the density of particles is too small. If we assume that minijet fragmentation is the leading production mechanism of

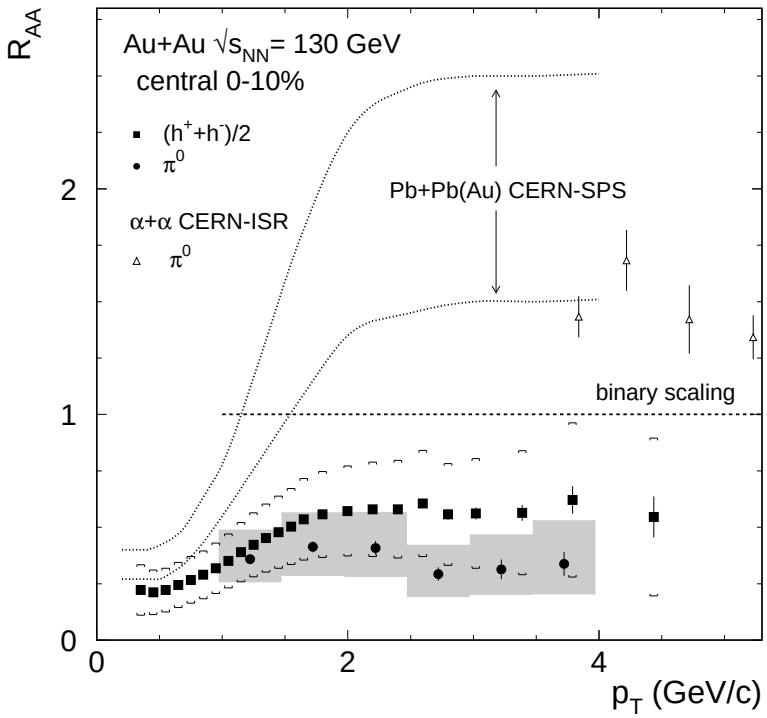

Figure 5. The ratio of transverse momentum distributions of charged hadrons and neutral pions in Au + Au and pp collisions at $\sqrt{s} = 130$ GeV; from [32].

high p_t particles, then the growth of the B/π ratio implies that minijet fragmentation is severely affected by the medium. Another scenario [34] attempts to explain both B/π puzzle and a large value of baryon asymmetry $\bar{B}/B \neq 1$, and invokes the contribution of non–perturbative gluonic junctions in nuclear collisions [35].

2.2.3. Charm production

The production of heavy flavors and quarkonia represents a very important and exciting part of RHIC program. While these studies will benefit in the future from increased luminosity and improvements in the detectors (allowing, in particular, to reconstruct the decay vertex of heavy hadrons), the first measurement of charm production cross section has been already reported [36]. This has been done by deciphering the charm decay contribution to the single electron spectrum – see Fig.6. Of particular interest is the fact that while the production cross sections of light hadrons, as discussed above, show strong nuclear effects, the cross section of charm production, within the error bars of the measurement, scales with the number of NN collisions. These results may imply much smaller, in comparison to light quarks, energy loss of heavy quarks [37] stemming from the suppression of the gluon radiation at small angles ("dead cone effect").

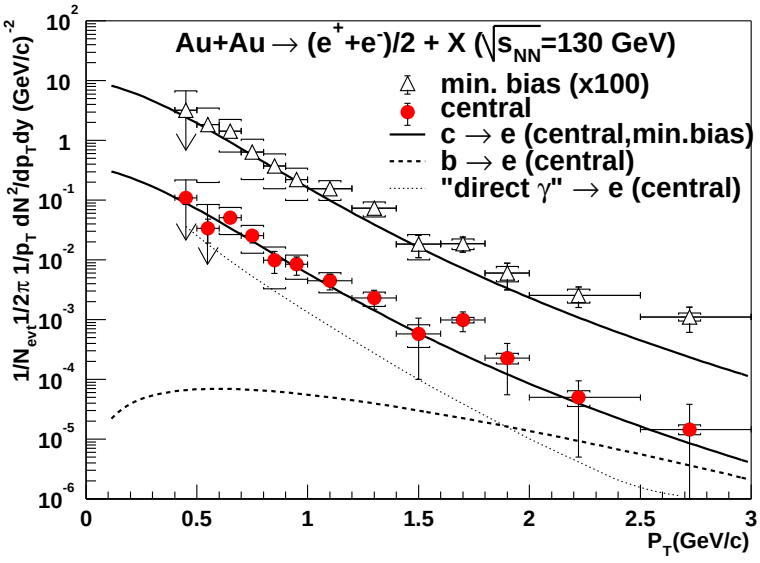

Figure 6. The background–subtracted electron spectra for minimum bias $(0-92\%)$ and central $(0-10\%)$ collisions compared with the expected contributions from open charm decays; from [36].

3. What have we learned so far?

It is too early to assess the implications of RHIC results; however, it is becoming increasingly clear that they challenge most, if not all, of the existing theoretical dogmas. A coherent and convincing theory describing all of the observed phenomena directly in terms of QCD still has to be born. However, we can already conclude that many of the observed phenomena clearly manifest collective behavior; nuclear collisions at RHIC are not an incoherent superposition of nucleon–nucleon collisions.

The measured particle multiplicities and transverse momentum spectra allow to estimate initial energy density at the early moments of the collision; a typical value inferred in this way is about 20 GeV/fm^3 (see, e.g., [9]). The dynamics of strongly interacting matter at such energy density (exceeding the energy density in a nucleus by over two orders of magnitude!) should be described in terms of quarks and gluons, and the collective phenomena observed at RHIC thus directly reflect the properties of high density QCD.

REFERENCES

1. D. J. Gross and F. Wilczek, Phys. Rev. Lett. **30** (1973) 1343.
2. H. D. Politzer, Phys. Rev. Lett. **30** (1973) 1346.
3. L. V. Gribov, E. M. Levin and M. G. Ryskin, Phys. Rept. 100, 1 (1983).
4. A. H. Mueller and J. w. Qiu, Nucl. Phys. B 268, 427 (1986).
5. J. P. Blaizot and A. H. Mueller, Nucl. Phys. B 289, 847 (1987).
6. L. McLerran and R. Venugopalan, Phys. Rev. D 49 (1994) 2233, 3352; D 50 (1994)

2225.
7. R. J. Glauber "High Energy Collision theory" in *Lectures in Theoretical Physics,* vol. 1, W. E. Brittin and L. G. Duham (eds.) Interscience, New York, 1959.
8. D. Kharzeev, C. Lourenco, M. Nardi and H. Satz, Z. Phys. C 74 (1997) 307 [arXiv:hep-ph/9612217].
9. D. Kharzeev and M. Nardi, Phys. Lett. B 507 (2001) 121 [arXiv:nucl-th/0012025].
10. V. A. Abramovsky, V. N. Gribov and O. V. Kancheli, Yad. Fiz. 18, 595 (1973) [Sov. J. Nucl. Phys. 18, 308 (1973)].
11. V. N. Gribov, Sov. Phys. JETP 29, 483 (1969) [Zh. Eksp. Teor. Fiz. **56**, 892 (1969)].
12. B. B. Back *et al.* [PHOBOS Collaboration], Phys. Rev. Lett. 88 (2002) 022302 [arXiv:nucl-ex/0108009].
13. B. B. Back *et al.* [PHOBOS Collaboration], Phys. Rev. C 65 (2002) 061901.
14. A. Bialas, M. Bleszynski and W. Czyz, Nucl. Phys. B 111 (1976) 461.
15. X. N. Wang and M. Gyulassy, Phys. Rev. Lett. 86 (2001) 3496 [arXiv:nucl-th/0008014].
16. S. y. Li and X. N. Wang, Phys. Lett. B **527** (2002) 85 [arXiv:nucl-th/0110075].
17. D. Kharzeev and E. Levin, Phys. Lett. B 523 (2001) 79 [arXiv:nucl-th/0108006].
18. I. G. Bearden *et al.* [BRAHMS Collaboration], Phys. Rev. Lett. 88 (2002) 202301 [arXiv:nucl-ex/0112001].
19. B. Zhang, C. M. Ko, B. A. Li and Z. w. Lin, Phys. Rev. C 61 (2000) 067901.
20. D. Kharzeev, R. D. Pisarski and M. H. Tytgat, Phys. Rev. Lett. 81 (1998) 512 [arXiv:hep-ph/9804221].
21. C. Adler *et al.* [STAR Collaboration], Phys. Rev. C 66 (2002) 034904.
22. D. Teaney, J. Lauret and E. V. Shuryak, Phys. Rev. Lett. 86 (2001) 4783.
23. P. F. Kolb, P. Huovinen, U. W. Heinz and H. Heiselberg, Phys. Lett. B 500 (2001) 232 [arXiv:hep-ph/0012137].
24. Y. V. Kovchegov and K. L. Tuchin, Nucl. Phys. A 708 (2002) 413.
25. A. Krasnitz, Y. Nara and R. Venugopalan, arXiv:hep-ph/0204361.
26. M. Gyulassy, I. Vitev, X. N. Wang and P. Huovinen, Phys. Lett. B 526 (2002) 301.
27. E. V. Shuryak, Phys. Rev. C 66 (2002) 027902 [arXiv:nucl-th/0112042].
28. C. Adler *et al.* [the STAR Collaboration], Phys. Rev. Lett. 86 (2001) 4778 [arXiv:nucl-ex/0104022].
29. J. D. Bjorken, FERMILAB-PUB-82-59-THY.
30. M. Gyulassy and X. n. Wang, Nucl. Phys. B 420, 583 (1994) [arXiv:nucl-th/9306003].
31. R. Baier, Y. L. Dokshitzer, A. H. Mueller, S. Peigne and D. Schiff, Nucl. Phys. B 483, 291 (1997) [arXiv:hep-ph/9607355].
32. K. Adcox *et al.* [PHENIX Collaboration], Phys. Rev. Lett. 88, 022301 (2002) [arXiv:nucl-ex/0109003].
33. K. Adcox *et al.* [PHENIX Collaboration], Phys. Rev. Lett. 88 (2002) 242301 [arXiv:nucl-ex/0112006].
34. I. Vitev and M. Gyulassy, Phys. Rev. C 65 (2002) 041902 [arXiv:nucl-th/0104066].
35. D. Kharzeev, Phys. Lett. B 378 (1996) 238 [arXiv:nucl-th/9602027].
36. K. Adcox *et al.* [PHENIX Collaboration], Phys. Rev. Lett. 88 (2002) 192303 [arXiv:nucl-ex/0202002].
37. Y. L. Dokshitzer and D. E. Kharzeev, Phys. Lett. B 519 (2001) 199 [arXiv:hep-

ph/0106202].